BIO-INSPIRED CONTROLLABLE ADHESIVE

Sathya S. Chary*, John W. Tamelier, Michael T. Northen, Kimberly L. Turner
Dept. of Mechanical Engineering, University of California, Santa Barbara
Santa Barbara, CA 93106

Jeffrey Trexler, Paul Rubel, Christopher Gudeman
Innovative Micro Technology
Santa Barbara, CA 93117

Jeffrey Pulskamp, Madan Dubey, Ronald Polcawich
U.S. Army Research Laboratory
Adelphi, MD 20783

ABSTRACT

Geckos, as well as many species of insect, have evolved a robust reversible adhesion mechanism, enabling them to traverse rough, smooth, vertical or inverted surfaces. The extraordinary climbing ability of geckos has been attributed to the fine structure of their toe pads which contain arrays of thousands of micron-sized setal stalks which are in turn terminated by millions of finger-like spatular pads having nano-scale dimensions. The hierarchical structure of the adhesive hairs provides several levels of compliance and enables them to come into close enough contact with rough surfaces to exploit the normally weak van der Waals force for strong adhesion. MEMS fabrication techniques are capable of producing micrometer and sub-micron features in a massively parallel fashion with a high degree of repeatability. This paper describes the use of such batch processing techniques to produce a synthetic reversible dry adhesive. A potential application for a controllable adhesive system capable of both strong attachment and rapid detachment clearly exists in the design of climbing robotic systems.

1. INTRODUCTION

The mechanism of adhesion in the gecko has been of scientific interest since Aristotle *(Thompson, 1918*). Since then scientific investigations have revealed much about the construction of the pad in the gecko's foot (*Williams and Peterson, 1992; Maderson, 1964*). Most recently there has been an intensifying scientific investigation into the fundamental physics of the adhesive, isolating van der Waals as the primary source of adhesion (*Autumn et al., 2000*), with additional evidence that humidity may also play an important role (*Huber et al., 2005*). Van der Waals interactions produce weak and short-range forces, therefore the gecko must create a large amount of intimate surface contact to have enough adhesion to hang from a vertical or inverted surface. The gecko accomplishes this with a highly compliant pad structure, which allows it to conform to surfaces, without creating a large amount of elastic repulsive force (*Persson and Gorb, 2003*).

The gecko adhesive is a multi-scale hierarchical structure composed of β-keratin (*Hiller, 1975*). While the nanostructures at the final termini of the system are of significant interest presently in the scientific community, it is the entire gecko system that is responsible for the superior clinging ability of the gecko. The gecko has four feet, each containing five digits. The toes themselves are very flexible, able to roll up and away from a surface – important for the release mechanism. Within each toe are rows of imbricated lamellae supported by blood sinuses in the pad of the tarsus – which act as a sort of hydraulic suspension. The lamellae contain rows of thin slender fibers, called setae, approximately 130 μm in length and 20 μm in diameter (*Hildebrand, 1988*), Fig.1. The terminus of each seta branches into thousands of smaller fibers, or spatular stalks. At the end of each of these stalks the structures flatten out into a flat 200 nm wide and 5 nm thick pad, or spatula (*Maderson, 1964; Hildebrand, 1988; Autumn et al., 2000*).

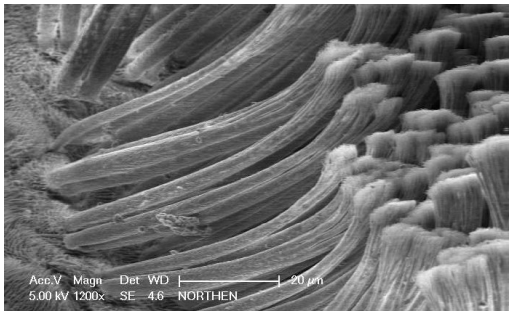

Fig.1. Micro-scale gecko setal arrays

Report Documentation Page

Form Approved
OMB No. 0704-0188

1. REPORT DATE	2. REPORT TYPE	3. DATES COVERED
DEC 2008	**N/A**	**-**

4. TITLE AND SUBTITLE	5a. CONTRACT NUMBER
Bio-Inspired Controllable Adhesive	5b. GRANT NUMBER
	5c. PROGRAM ELEMENT NUMBER
6. AUTHOR(S)	5d. PROJECT NUMBER
	5e. TASK NUMBER
	5f. WORK UNIT NUMBER
7. PERFORMING ORGANIZATION NAME(S) AND ADDRESS(ES) **Dept. of Mechanical Engineering, University of California, Santa Barbara Santa Barbara, CA 93106**	8. PERFORMING ORGANIZATION REPORT NUMBER
9. SPONSORING/MONITORING AGENCY NAME(S) AND ADDRESS(ES)	10. SPONSOR/MONITOR'S ACRONYM(S)
	11. SPONSOR/MONITOR'S REPORT NUMBER(S)

12. DISTRIBUTION/AVAILABILITY STATEMENT
Approved for public release, distribution unlimited

13. SUPPLEMENTARY NOTES
See also ADM002187. Proceedings of the Army Science Conference (26th) Held in Orlando, Florida on 1-4 December 2008, The original document contains color images.

14. ABSTRACT

15. SUBJECT TERMS

16. SECURITY CLASSIFICATION OF:			17. LIMITATION OF ABSTRACT	18. NUMBER OF PAGES	19a. NAME OF RESPONSIBLE PERSON
a. REPORT	b. ABSTRACT	c. THIS PAGE			
unclassified	**unclassified**	**unclassified**	**UU**	**7**	

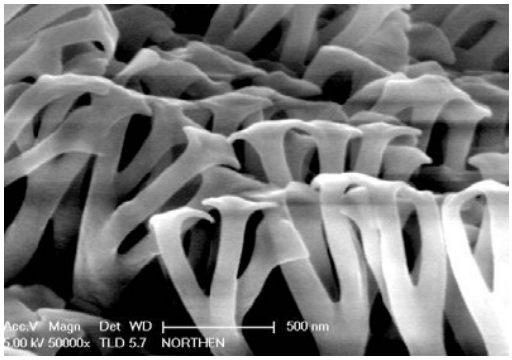

Fig.2. Nano-scale spatulae on gecko setae

As with any adhesive, in order for the adhesive to work it has to come into contact with the adhering surface. For an ideally smooth surface making contact is relatively straightforward. However, the gecko does not have the luxury of ideal surfaces in nature. The first thing the gecko is able to do is bend its legs, adjusting for the curvature of the trunk, putting the pads into contact with the surface. Depending on the surface, the toes are then able to bend and wrap around any centimeter scale roughness. Next the blood sinuses in the pad are able to deform to millimeter scale roughness in the surface. The setae are then able to bend and nestle into milli to micro-scale roughness, which then puts the spatulas into contact with the surface. The thin, compliant spatulas are then able to conform to nanoscale roughness and make intimate contact with the surface.

As will be discussed in the adhesion mechanics section, this intimate contact is necessary to enhance the van der Waals interactions responsible for adhesion. Prior work in this area has focused solely on fabricating nanostructured surfaces (*Autumn et al., 2002; Geim et al., 2002; Sitti, 2003; Sitti and Fearing, 2003*). However, it is clear that the hierarchical nature of the gecko adhesive serves many other purposes as well – e.g. enhancing surface conformation and inducing a frictional component. In this work, efforts have been focused on creating the first two levels of the hierarchical structure. That is creating an analogue to the spatular/setal structure by integrating similar nano/micro-scale structures.

2. ADHESION MECHANICS

The simplest relevant case to consider is a sphere contacting a flat surface. Hertz found that a sphere contacting a flat, smooth surface (assuming the materials to be homogeneous and isotropic) has a contact area of (*Hertz, 1862*):

$$A_c = \pi\left(\frac{RF_n}{K}\right)^{\frac{2}{3}} \tag{1}$$

Where R is the radius of the sphere, F_n the normal force, and K is the effective elastic modulus given by:

$$\frac{1}{K} = \frac{3}{4}\left(\frac{1-\upsilon_1^{\,2}}{E_1} + \frac{1-\upsilon_2^{\,2}}{E_2}\right) \tag{2}$$

Where E_i and ν_i are the Young's moduli and Poisson's ratios of the two materials respectively.

In this case Hertz assumes that the sphere is pushed into the surface, deforms, and then when the force is removed returns back to original configuration without hysteresis. While this theory explains the contact mechanics it does not predict adhesion between the sphere and the flat surface. Johnson-Kendall-Roberts considered the surface energies of the contacting surfaces and found that the contact area increases due to a reduction in interfacial energy (*Johnson et al., 1971*) given by equation (3) below:

$$A_c = \pi\left[\frac{R}{K}\left(F_n + 6\pi R + \sqrt{12\pi\gamma RF_n + \left(6\pi\gamma R\right)^2}\right)\right]^{\frac{2}{3}}$$

where γ is the interfacial energy and responsible for the mechanism of adhesion.

A significant outcome is that even in the absence of a normal force there is a contact area and an adhesive force. The radius of contact is given by:

$$a_o = \left(\frac{12\pi\gamma R^2}{K}\right)^{\frac{1}{3}} \tag{4}$$

And the pull-off force, or magnitude of adhesion is:

$$F_{JKR} = 3\pi\gamma R \tag{5}$$

Considered a short-range molecular interaction force, van der Waals forces arise from temporarily induced dipoles between two neutral molecules. The momentary shift in the electron cloud of one molecule induces the shift of a neighboring molecule's cloud of electrons. The two dipoles then attract each other. These London dispersion forces operate over a short range, typically <10 nm, and can be described using a Leonard-Jones potential $\psi(d)$ (*Israelachvili, 1991*)

$$\psi(d) = \psi_o\left[\left(\frac{d^*}{d}\right)^{12} - \left(\frac{d^*}{d}\right)^{6}\right] \tag{6}$$

where ψ_o is the strength of the interaction, d* the range of the interaction and d the distance of the two molecules. The positive portion of the equation denotes the repulsive energy associated with two molecules not being able to penetrate each other. The force is very strong, but also very short ranged.

The concept of contact splitting in the gecko adhesive system offers a direct explanation for the increase in adhesion observed when many small contacts are made as opposed to one large contact. A theory developed by *Arzt et al.* (*2003*) shows how the size of the final termini of an animal's contacts is inversely related to the mass of the animal, Fig. 3. For example the largest animal to use this adhesion system, the Tokay Gecko, also has the smallest termini, ~200 nm, whereas a fly has termini of order 2 µm.

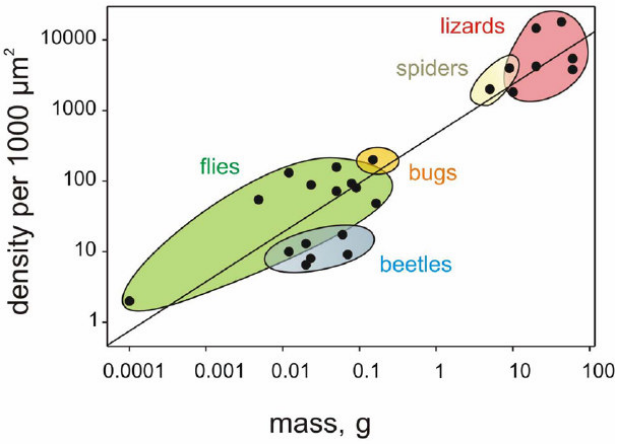

Fig.3. Illustration of the contact splitting phenomenon in nature

This phenomenon can be understood by inspection of Eq. (5), which shows that the JKR adhesion force is proportional to a linear dimension of the contact; therefore, by splitting up the contact into *n* subcontacts (setae), each with radius $R/\sqrt{n}$ the total adhesion force is increased to:

$$F_{JKR}(n) = \sqrt{n}3\pi\gamma R \tag{7}$$

Thus, contact splitting is able to offer an explanation for the fine terminal structure of the fine hair attachment system. There is however much more to the structure of the adhesive system. The fine hairs are located at the end of long, 130 µm, slender, 20 µm, setal stalks. These stalks are attached to the foot of the gecko via an undulated surface cushioned by blood sinuses. In view of contact mechanics, this hierarchical system seems to aid in increasing surface contact with non-ideal surfaces.

In the case of rough surfaces, it is no longer possible to assume that a single large contact will make perfect contact with a surface. In addition it is not possible to assume that if a large contact is split into many smaller contacts they will all make contact. For a rough surface it becomes very important to consider the roughness and the ability of the two surfaces to make intimate contact. Thus, the mechanical properties of the underlying substrate become important. If one substrate is highly compliant then the surfaces will mate better and adhesion will be increased (*Hui et al., 2005*). The long slender setae aid in surface conformation increasing contact area without increasing the repulsive push-off force. This push-off force can be modeled as an elastic restoring force:

$$F_{adhesion} = F_{attraction} - F_{elastic} \tag{8}$$

The concept of reducing the elastic restoring force and enhancing surface conformation was a driving force for the work presented here. This work was the first effort to create a hierarchical structure; the first work to integrate two different scales of structures (micro and nano) for enhanced adhesion.

From the above, it is clear that adhesion is related to the amount of contact area between surfaces. A few general rules can be made about adhesion accordingly:

1. Adhesion increases with decreasing surface roughness.

2. Soft, flexible and conformal surfaces increase adhesion.

3. Deformable surfaces conform to surface roughness making intimate contact and enhancing adhesion.

4. Surface conformation can also be enhanced by increasing the normal loading force

In summary, the adhesion mechanics of the fine hair adhesive system relies on a large number of weak, short-range interactions to create a large amount of adhesion. The fundamental interaction seems to be a van der Waals force, while it may still be possible that water plays a role through other effects. Using JKR contact mechanics, it is possible to demonstrate the improved adhesion due to contact splitting. Just as important as the contact mechanics at the nanoscale is the compliance of the surface at the micro and mesoscales.

3. FABRICATION

The bio-mimetic adhesive system developed is composed of flexible nickel paddles coated with vertical

aligned polymeric nano-rods *(Northen et al., 2008)*. The micrometer-scale paddles and nanometer-scale polymeric rods provide two levels of structural hierarchy for increased surface contact. The nano-rods are treated with a hydrophobic coating to prevent self-adhesion and bunching, thereby increasing robustness and reusability. The ferromagnetic properties of nickel enable the use of a magnetic field to reorient the paddles in an unfavourable configuration facing away from a contacting surface, reducing adhesion by a factor of 40.

Released 150 nm thick and 130 μm long nickel structures (Fig. 4), coated with aligned vertical arrays of stiff polymeric nano-rods ~200 nm in diameter and ~3 μm tall (Fig. 5), were fabricated using a combination of compatible massively parallel fabrication techniques. First, the nickel cantilever microstructures were photolithographically defined with a standard lift-off deposition scheme. Then the nickel pattern was transferred into the exposed silicon and undercut for release using the Bosch deep reactive ion etch process. The remaining photoresist coating on the cantilever platforms was then exposed to an oxygen plasma with an applied bias between wafer and plasma, creating nano-rods aligned orthogonally to the surface, with an aspect ratio of ~15. Post organorod growth, surface property modification was achieved by fluorocarbon deposition using the passivation step in a PlasmaTherm Bosch process tool. Running a 9 second deposition would deposit roughly 30 nm of fluorocarbon on the surface of the organorods. The hydrophobic coating switched the organorod surface from hydrophilic to highly-hydrophobic with a contact angle of 154° (Fig. 7).

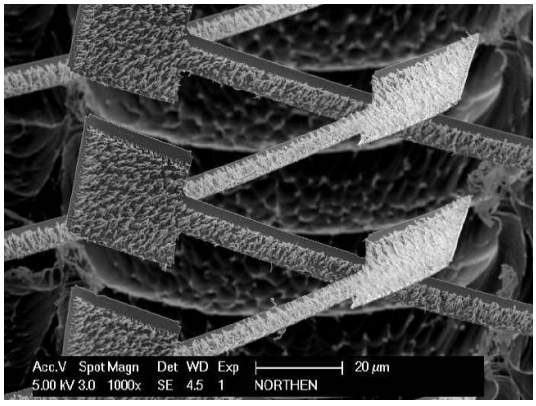

Fig.4. Ferromagnetic nickel paddles coated with nanorods

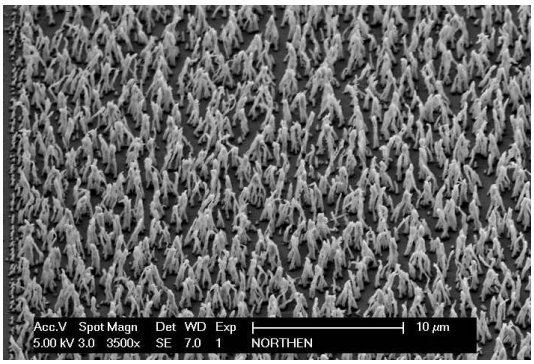

Fig.5. SEM of polymeric nanorods

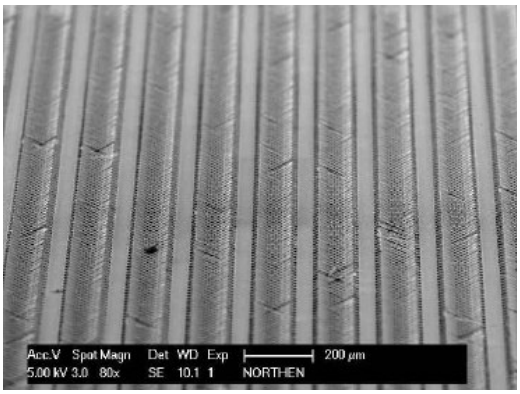

Fig.6. MEMS fabrication techniques make massively parallel arrays using the technology possible

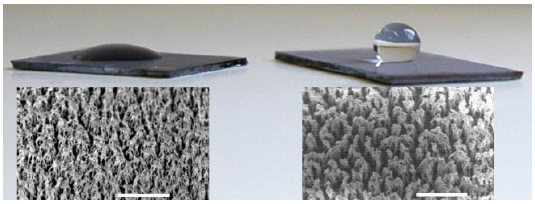

Fig.7. Switch to hydrophobicity on deposition of C_xF_y passivation polymer layer

Subjected to a magnetic field, the platforms rotate to align themselves with the magnetic field lines. The rotation leaves the edge of the platforms facing in the normal direction and the "sticky" face to the side (Fig.8). Thus when a surface approaches from the normal direction it only contacts the edges of the platforms. Since the edges of the platforms provide very little surface area, and have no nanorod coating, very little adhesion is produced. A reversible dry adhesive based on complaint hierarchical structures to exploit van der Waals forces has thus been fabricated.

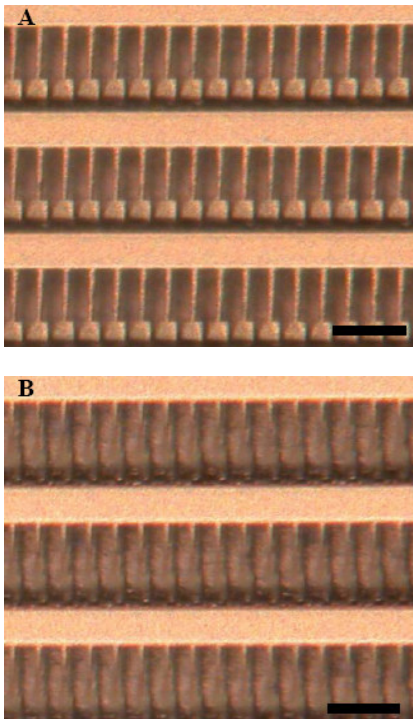

Fig.8. Orientation of ferromagnetic paddles with the magnetic field turned OFF (A, top) and with the field turned ON (B, bottom)

4. ADHESION TESTING

The structures were characterized *(Northen et al., 2008)* using a home-built adhesion test apparatus (Basalt-II) with C. Greiner and E. Arzt at the Max Planck Institute for Metals Research, Germany. Fig. 9 (*Peressadko and Gorb, 2004*) shows a schematic of the apparatus. The basic operating principle of the system is similar to an atomic force microscope, but implemented on a larger scale: the deflection of a glass spring is monitored, using laser interferometry, to determine the forces applied to the spring tip. This tip was a glass flat punch of 5 mm diameter. In order to ensure proper alignment between the tip and the sample, the tip was attached to the cantilever with high-strength glue while in intimate contact with the sample stage.

Test samples were placed on the micropositioning stage and moved to near contact with the spring tip. The tip was then lowered using a piezo electric actuator, and proper alignment was ensured through a horizontally oriented stereomicroscope. Actuation of the probe and data collection was performed using an automated National Instruments LabView™ program. Through calibration of the cantilever (spring constant, k=137.1 N/m) it was possible to determine the interaction forces between the flat punch tip and the test surface. Upon withdrawal from the surface, adhesion produced a characteristic pull-off event, evident in a negative dip of the force-displacement curve. The reversible adhesive was tested with and without Neodymium Iron Boron ($Nd_2Fe_{14}B$) rare earth metal magnet below the silicon chip.

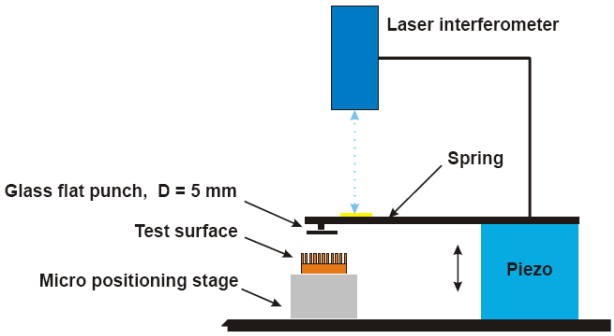

Fig.9. Schematic of the adhesion test apparatus

While the gecko setae and spatulae are composed of β-keratin, here a combination of photoresist, silicon and nickel was used to create a 3-dimensional structure actuated through the application of a magnetic field. The photoresist (E = 6.2 +/- 0.2 GPa) is transformed into 200 nm diameter 3 μm tall nanorods, analogous to the β-keratin [E = 1-15 GPa (*Sitti and Fearing, 2003*)], spatulae of the gecko. These nanorods coat the thin nickel beams and act to enhance adhesion through contact splitting and nanoscale roughness conformation – thus acting as the active portion of the adhesive. The 150 nm thick nickel beams aid in surface conformation (just as the setae in the gecko) and as a deactivation mechanism for the adhesive. The stress mismatch between the photoresist and nickel causes the cantilevers to bend away from the surface. The upwards bend of these beams gives added compliance to a rough test surface by allowing individual cantilevers to bend and conform long before the test surface makes contact with the rigid adhesive substrate. In addition, the upwards bending of the beams isolates the active portion of the adhesive from the substrate.

With the active portion of the adhesive isolated, the properties of the adhesive could then be controlled by actuating the platforms. High-aspect-ratio ferromagnetic structures have been shown to rotate within a magnetic field to align their long axis with the magnetic field vector (*Judy et al., 1995*). When the structures were placed on top of a permanent magnet the paddles were observed to rotate about their long axis, Fig. 6. This rotation is attributed to the preferential alignment of the long axis of the width of the pad in the magnetic field.

5. RESULTS

Adhesion testing of the flexible cantilevered structures, without an applied magnetic field, produced unloading curves with a characteristic pull-off event shown in figure 10 (upper curve). The pull-off force was observed to vary with the maximum applied normal load (due to slight misalignments between the flat punch and the test surface) until a saturation adhesion strength of ~14 Pa was observed (obtained by dividing the adhesion force by the projected area of all pad surfaces), Fig. 11.

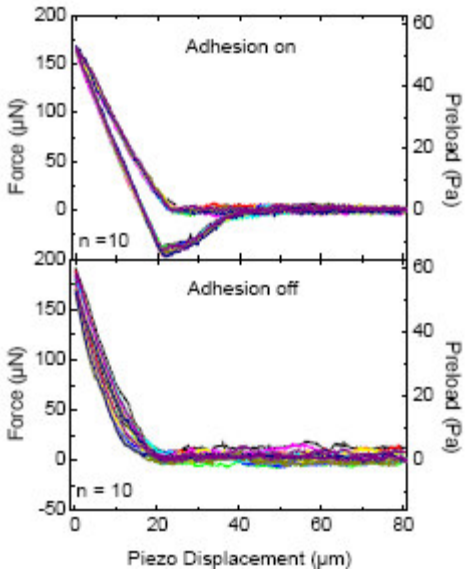

Fig.10. Representative adhesion test data

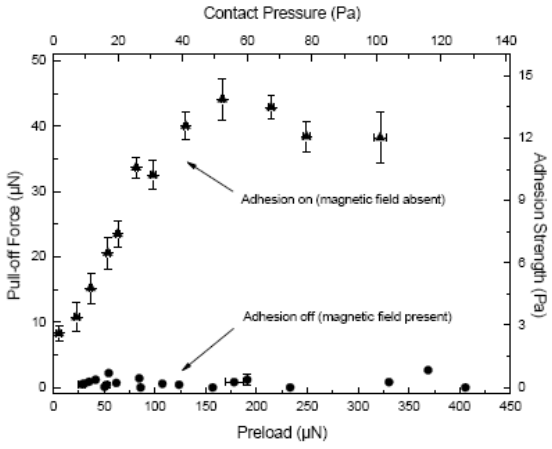

Fig.11. Adhesion results showing the on/off behavior of the structures with and without an applied magnetic field

Strength values in the graphs were obtained by dividing the interaction force by the contact area of the paddles. In the 'ON' state, the devices showed an initial increase in adhesion with preload force, characteristic of increased surface contact with applied load (likely a result of slight misalignment between the 5 mm flat punch and test surface). Error bars represent 10 data sets at a specified displacement with no omission of outliers.

Upon withdrawal from the surface, adhesion produced a characteristic pull-off event, evident in a negative dip of the force-displacement curve. The reversible adhesive was tested, both with and without a rare earth magnet below the silicon chip. In contrast to the adhesion seen in a rest state, the application of a magnetic field to the structures produced a catastrophic loss of adhesion. The minimum negative force detected was 0.37 ± 0.28 Pa (compared with 14 Pa without a magnetic field). For no tests on the structures with an applied magnetic field was there an observable pull-off incident. When the structures were placed on top of a permanent magnet the paddles were observed to rotate about their long axis. The large rotation induced by the magnetic field causes the paddles to turn sideways, concealing the active portion of the adhesive from the test surface. Thus when a surface approaches from the normal direction it only contacts the edges of the platforms. Since the edges of the platforms provide very little surface area and have no nano-rod coating, very little adhesion is produced – less than the noise in the instrumentation.

6. DISCUSSION

In addition to the decarease in active surface area on applying a magnetic field, a decrease in surface compliance was seen in the structures with an applied magnetic field. The twisting of the cantilevers increases the second moment of area of the structures, relative to the indenting tip, increasing the stiffness and consequently reducing the compliance of the system. Ultimately, the sideways turned paddles will contact the underlying substrate and statically block an adhering surface from contacting the support substrate – completely turning off adhesion.

As discussed earlier, a saturation adhesion strength of ~14 Pa was observed. It should be noted that this is a purely adhesive measurement testing in the normal pull-off direction, whereas reported values for the gecko test in the transverse frictional direction (*Autumn, 2006*), making comparisons between the two systems tenuous.

Alignment issues, surface inconsistencies and unknown probe geometries have presented difficulties in quantification of this new class of bio-inspired non-pressure-sensitive-adhesives. One suggested metric is to simply divide the adhesion force by the maximum preload force, $\mu' = F_{adhesion}/F_{preload}$ (*Autumn, 2006*). In this system the maximum μ' value was found to be 1.47 +/- 0.4, occurring at the minimum pre-load with an observable pull-off event (limited by the noise level of the instrumentation). This value offers a substantial increase from previous synthetic work with μ' values of 0.125 (*Northen and Turner, 2005*) and 0.06 (*Geim et al., 2003*), but still falls short of the gecko with μ' = 8 to 16 (*Autumn, 2006*).

7. CONCLUSIONS

A novel approach has been presented for creating a synthetic analogue to the gecko adhesive system. The hierarchical system is composed of aligned vertical nanorods coating flexible micron scale cantilever paddles. The paddles, composed of nickel, rotate when subjected to a magnetic field. This rotation conceals the nanostructures on the paddle surface and greatly reduces the available surface area for adhesion. Testing of the system showed reversible adhesion behavior switching from a μ' value ($F_{adhesion}/F_{preload}$) of 1.47 +/- 0.4 (largest reported value for a biomimetic system to date (*Autumn, 2006*)) to less than the noise level in the instrumentation. Thus an active hierarchical structure has been fabricated and demonstrated to display controlled and reversible adhesion. Further development of switchable adhesives will find applications ranging from everyday consumer products such as latching and fastening systems; to high-tech applications, such as enabling microrobotics to explore extraterrestrial surfaces or harsh climates otherwise not accessible to man.

Current work is also focusing on the frictional enhancement of adhesion. Here a friction force is applied by the electro-thermal actuator such that the nano-rods are sheared. A large fraction of the work of the actuator is combined with the work of adhesion when the nano-rods are sheared to angles >20°, where a significant fraction of the vector shear force is directed normally to the surface and thus increases the net adhesion. Future work will focus on extending the principles used to develop the magnetic response adhesive – involving optimization of individual components and integrating them into an overall robotic system.

REFERENCES

Aristotle (translated by Thompson), 350 B.C.E. (1918): Historia animalium, *D'A.W. (Oxford, The Clarendon Press)*, pp. 584.

E. Arzt, S. Gorb, R. Spolenak, 2003: *Proc. Natl. Acad. Sci USA* **100**, 10603.

K. Autumn et al., 2000: *Nature* **405**, 681.

K. Autumn et al., 2002: *Proc. Natl. Acad. Sci. USA* **99**, 12252.

K. Autumn, 2006: *Biological Adhesives* (Springer Verlag).

A. K. Geim, S. V. Dubonos, I. V. Grigorieva, K. S. Novoselov, A. A. Zhukov, 2003: *Nature Materials* **2**, 461.

H. Hertz, 1862: *Reine und Angewandte Mathematik* **92**, 156.

M. Hildebrand, 1988: *Analysis of Vertebrate Structure* (John Wiley & Sons, Inc, New York, ed. 3rd), pp. 701.

U. Hiller, 1975: *Journal of the Bombay Natural History Society* **73**, 278.

G. Huber et al., 2005: *PNAS* **102**, 16293.

C. Y. Hui, N. J. Glassmaker, A. Jagota, 2005: *The Journal of Adhesion* **81**, 699.

J. N. Israelachvili, 1991: *Intermolecular and Surface Forces* (Academic Press, London, ed. 2nd)

K. L. Johnson, Kendall, K., and Roberts, A. D., 1971: *Proc. Roy. Soc. Lond. A* **324**, 301.

J. Judy, R. Muller, H. H. Zappe, 1995: *Journal of Microelectromechanical Systems* **4**, 162.

P. F. A. Maderson, 1964: *Nature* **203**, 780.

M. T. Northen, K. L. Turner, 2005: *Nanotechnology* **16**, 1159.

M. T. Northen, C. Greiner, E. Arzt, K. L. Turner, 2008: *Advanced Materials* **2008**, 20, 1-5.

A. Peressadko, S. N. Gorb, 2004: *Journal Of Adhesion* **80**, 247.

B.N.J. Persson, S. Gorb, 2003: *Journal of Chemical Physics* **119**, 11437.

M. Sitti, 2003: Proceedings of the 2003 IEEE/ASME International Conference on Advanced Intelligent Mechatronics AIM 2003, Piscataway, NJ, USA.

M. Sitti, R. S. Fearing, 2003: *Journal of Adhesion Science and Technology* **17**, 1055.

E. E. Williams, J. A. Peterson, 1982: *Science* **215**, 1509.